Electronic Supplementary Material (ESI) for Dalton Transactions.

Electronic Supporting Information

Syntheses, Crystal-Solution Structures and Magnetic Properties of a Series of Decanuclear Heterometallic $[Ln^{III}_2Co^{II}_4Co^{III}_4]$ (Ln= Eu, Gd, Tb, Dy) Clusters

You-Zhu Yu,[a] Yue-Qiao Hu,[b,*] Yu-Hua Guo,[a] Yong-Sheng Niu,[a] Li-Guo Yang,[a] Hai-Xiang Song,[a] Yan-Hong Shen,[a] Xiao-Ming Zheng,[a] Shao-Gang Hou,[a] Guo-Dong Feng[b,*]

[a]College of Chemistry and Environmental Engineering, Anyang Institute of Technology, Anyang, Henan 455000, China.

[b]Key Laboratory of Advanced Molecular Engineering Materials, College of Chemistry and Chemical Engineering, Baoji University of Arts and Sciences, No. 1, Hi-Tech Avenue, Baoji 721013, China.

Table S1. Crystal data and structure refinement summary for **1-4**.

	1	**2**	**3**	**4**
Formula	$C_{42}H_{106}Cl_{14}Co_8Eu_2N_8O_{34}$	$C_{42}H_{106}Cl_{14}Co_8Gd_2N_8O_{34}$	$C_{40}H_{100}Cl_4Co_8Tb_2N_8O_{34}$	$C_{42}H_{102}Cl_4Co_8Dy_2N_8O_{34}$
Formula weight	2184.53	2195.08	2168.35	2201.55
Crystal system	Triclinic	Triclinic	Triclinic	Triclinic
Space group	*P*-1	*P*-1	*P*-1	*P*-1
a (Å)	11.6459(13)	11.5808(4)	11.5752(12)	11.604(8)
b (Å)	13.2464(14)	13.1176(5)	13.2401(13)	13.227(9)
c (Å)	14.6900(15)	14.5614(5)	14.6104(14)	14.653(9)
α (°)	72.037(4)	71.009	71.846(4)	72.181(7)
β (°)	67.296(4)	67.615	67.999(4)	67.638(7)
γ (°)	66.086(4)	65.536	65.542(4)	65.939(7)
V (Å^3)	1879.8(3)	1824.40(12)	1857.0(3)	1.869(2)
Z	1	1	1	1
ρ_{calcd} (g cm^{-3})	1.933	1.998	1.939	1.956
F(000)	1100	1098	1082	1098
μ (mm^{-1})	3.586	3.793	3.844	3.928
Collected reflections	50431	15699	49120	26311
Unique reflections	6567	6407	6482	6499
*R*int	0.0474	0.0291	0.0386	0.0496
Goodness-of-fit (GOF)	1.028	1.057	1.046	1.061
R_1 ($I > 2\sigma(I)$)[a]	0.0564	0.0492	0.0672	0.0506
*wR*2 (all data)[b]	0.1587	0.1448	0.1514	0.1447
$\rho_{maximum}/\rho_{minimum}$ (e Å^{-3})	4.829/ -1.237	5.158/-1.564	4.208/ -2.668	3.926/-1.686

[a] $R = \Sigma(||F_o| - |F_c||)/\Sigma|Fo|$. [b] $wR = [\Sigma w(|F_o|^2 - |F_c|^2)^2/\Sigma w(F_o{}^2)^2]^{1/2}$, where F_o = observed and F_c = calculated structure factors, respectively.

Table S2. Selected bond distances (Å) for **1**-**4**.

1			
Eu(1)-O(12)	2.324(4)	Co(1)-O(2)	1.890(5)
Eu(1)-O(2)	2.404(5)	Co(1)-N(2)	1.925(6)
Eu(1)-O(5)	2.434(5)	Co(1)-O(4)	1.935(5)
Eu(1)-O(16)$^{\#1}$	2.438(6)	Co(2)-O(12)	2.046(5)
Eu(1)-O(6)	2.453(5)	Co(2)-O(12)#2	2.054(5)
Eu(1)-O(3)	2.497(5)	Co(2)-O(3)#1	2.193(5)
Eu(1)-O(4)	2.525(5)	Co(3)-O(5)	1.880(5)
Eu(1)-O(8)	2.534(5)	Co(3)-N(4)	1.929(7)
Eu(1)-O(13)	2.623(5)	Co(4)-O(9)	2.059(5)
2			
Gd(1)-O(11)$^{\#1}$	2.312(4)	Co(1)-O(13)	1.889(4)
Gd(1)-O(5)	2.400(4)	Co(1)-O(2)	1.899(4)
Gd(1)-O(14)	2.417(5)	Co(1)-N(4)	1.920(5)
Gd(1)-O(13)	2.429(4)	Co(2)-O(1)	2.057(4)
Gd(1)-O(3)	2.435(4)	Co(2)-O(2)	2.162(4)
Gd(1)-O(6)	2.465(4)	Co(3)-O(5)	1.893(4)
Gd(1)-O(4)	2.499(4)	Co(3)-N(2)	1.920(6)
Gd(1)-O(2)	2.507(4)	Co(4)-O(11)#1	2.043(4)
Gd(1)-O(9)	2.599(5)	Co(4)-O(4)	2.151(4)
3			
O(7)-Tb(1)	2.423(12)	Co(1)-O(4)	1.892(8)
O(3)-Tb(1)	2.474(9)	Co(1)-O(2)	1.920(8)
O(4)-Tb(1)	2.392(8)	Co(1)-N(2)	1.929(11)
O(10)-Tb(1)	2.411(8)	Co(2)-O(5)	2.057(8)
O(11)-Tb(1)	2.439(8)	Co(2)-O(1)	2.163(8)
O(13)-Tb(1)	2.492(8)	Co(3)-O(10)	1.882(9)
O(14)-Tb(1)	2.620(10)	Co(3)-N(4)	1.935(11)
Tb(1)-O(5)$^{\#1}$	2.305(8)	Co(4)-O(14)	2.057(9)
O(1)-Tb(1)	2.505(8)	Co(4)-O(9)	2.076(10)
4			
Dy(1)-O(9)	2.297(5)	Co(1)-O(9)	2.058(6)
Dy(1)-O(12)	2.378(6)	Co(1)-O(8)	2.088(7)
Dy(1)-O(7)	2.403(8)	Co(2)-O(10)	1.941(6)
Dy(1)-O(4)	2.404(6)	Co(2)-N(3)	1.963(8)
Dy(1)-O(5)	2.421(6)	Co(3)-O(4)	1.880(6)
Dy(1)-O(13)	2.463(6)	Co(3)-N(2)	1.928(9)
Dy(1)-O(3)	2.512(6)	Co(3)-O(5)	1.915(6)
Dy(1)-O(6)	2.624(7)	Co(4)-O(2)	2.060(6)
Co(1)-O(10)$^{\#1}$	2.163(6)	Co(4)-Cl(1)	2.369(4)

Symmetry codes: for **1,** #1: -x+2,-y,-z; for **2**, #1: -x+1,-y+1,-z; for **3,** #1: -x+1,-y+2,-z+1; for **4,** #1: -x+1,-y+1,-z+1.

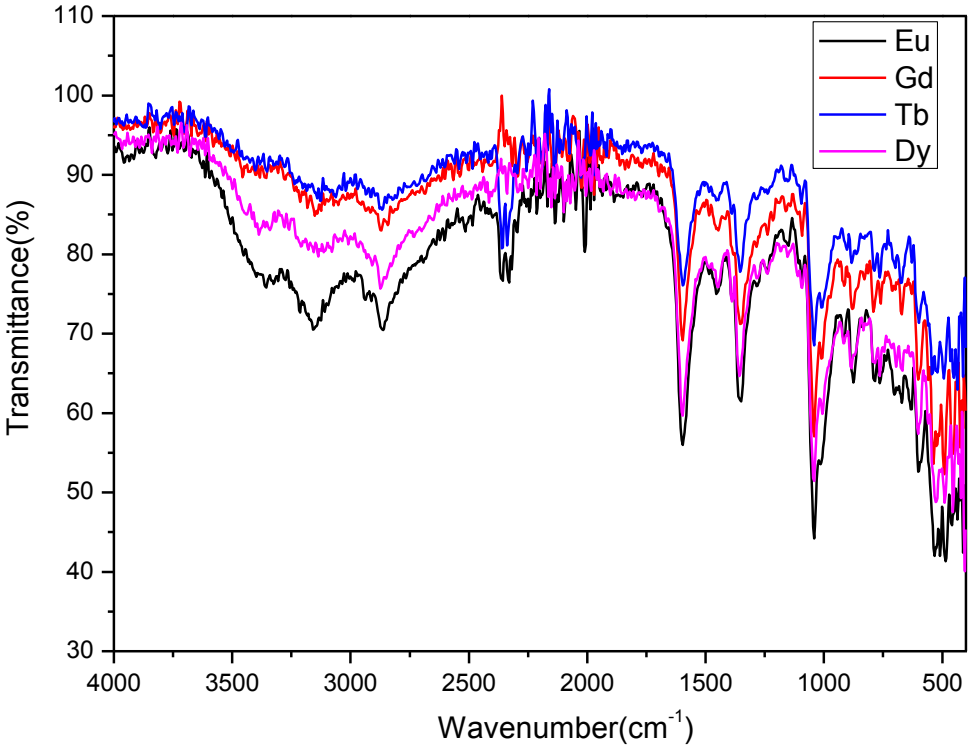

Fig. S1 IR spectra of **1-4**.

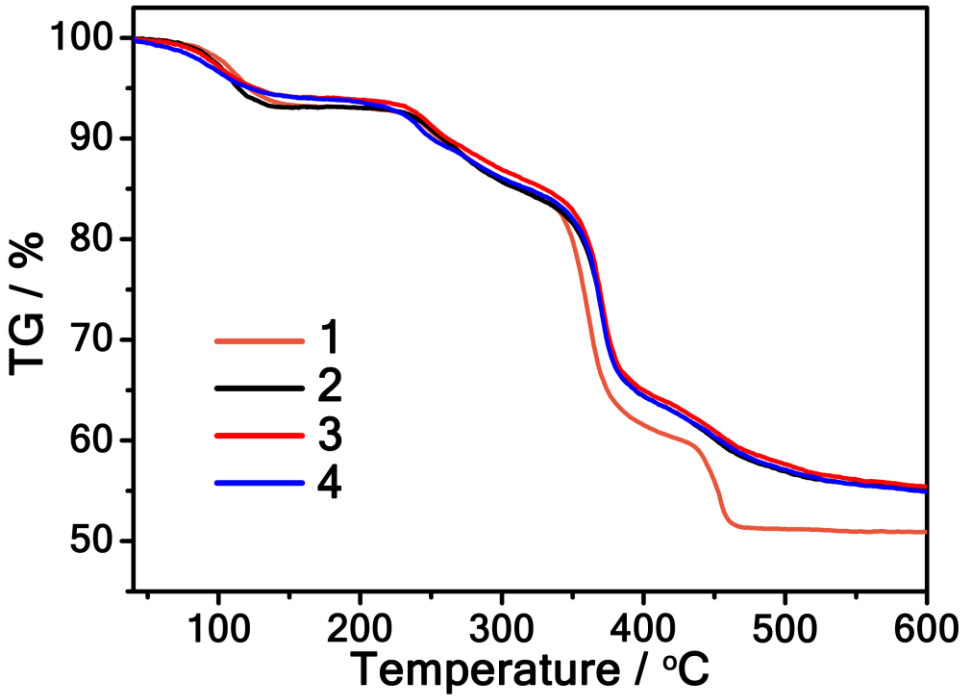

Fig. S2 TG curves for compounds **1-4**.

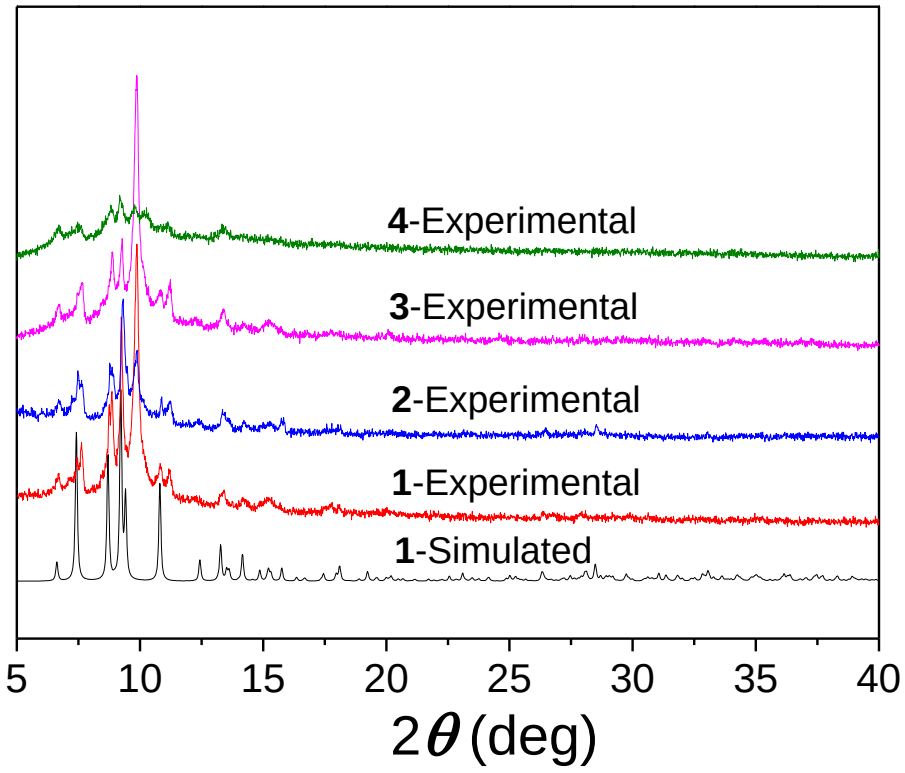

Fig. S3 X-ray powder diffraction (XRPD) patterns of **1-4** measured in air, respectively.

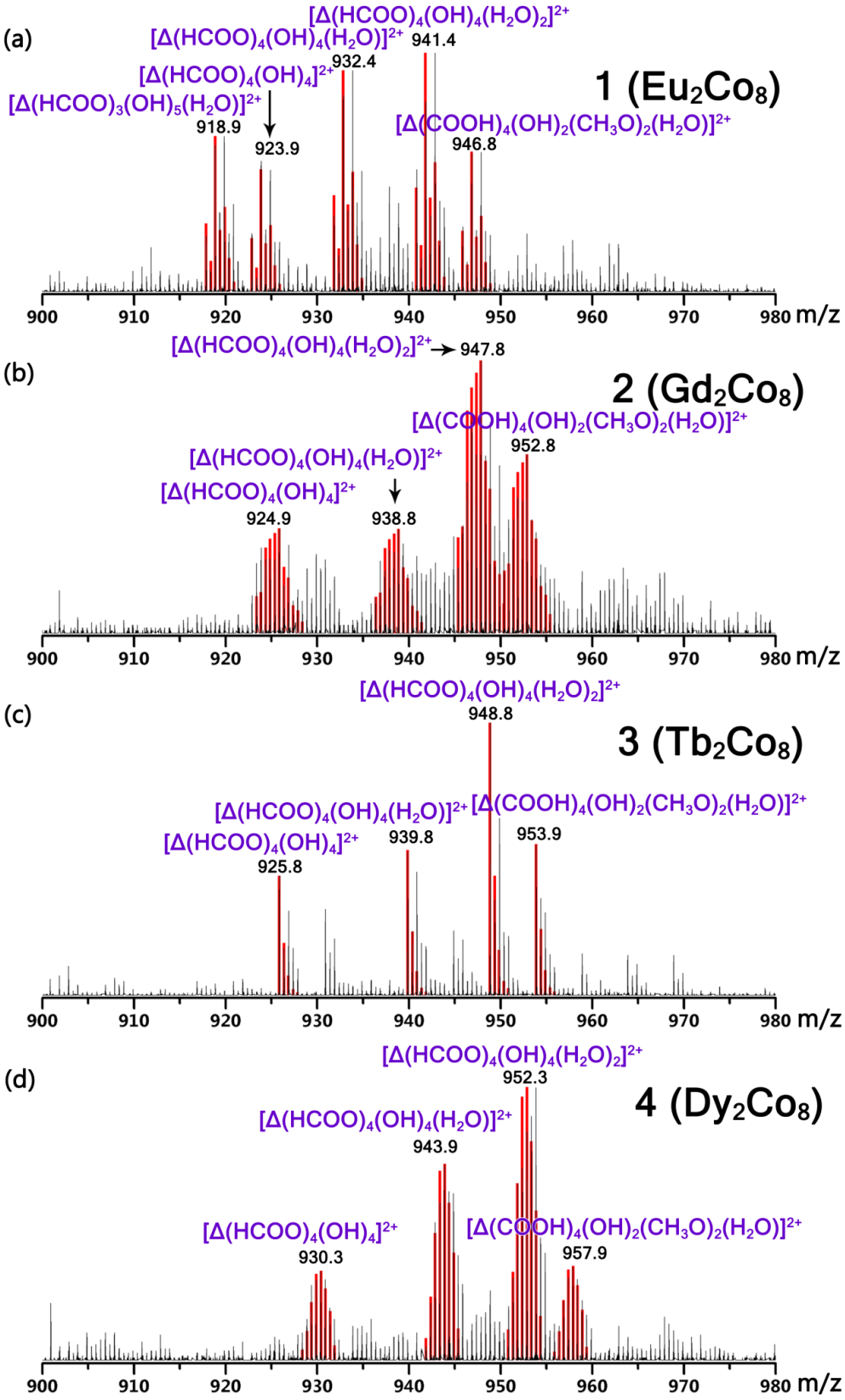

Fig. S4 Experimental ESI-MS (black line) and simulated (red line) data of **1**-**4**.

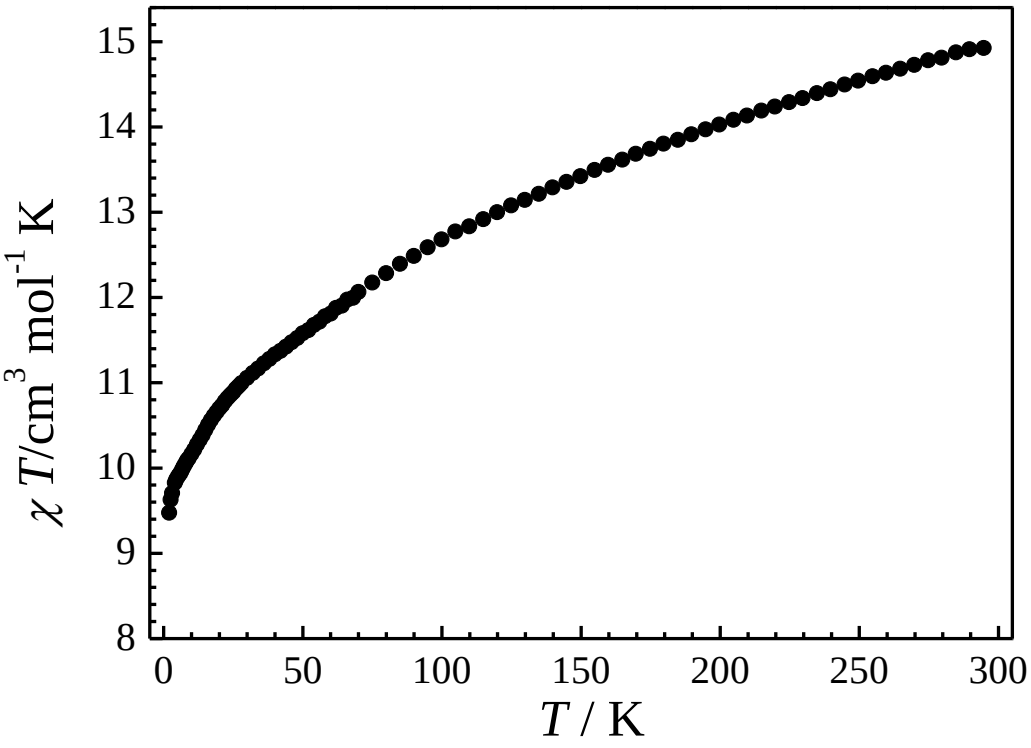

Fig. S5 Temperature dependence of $\chi_M T$ from 300-2K for **1** measured in a field of 2000 Oe.

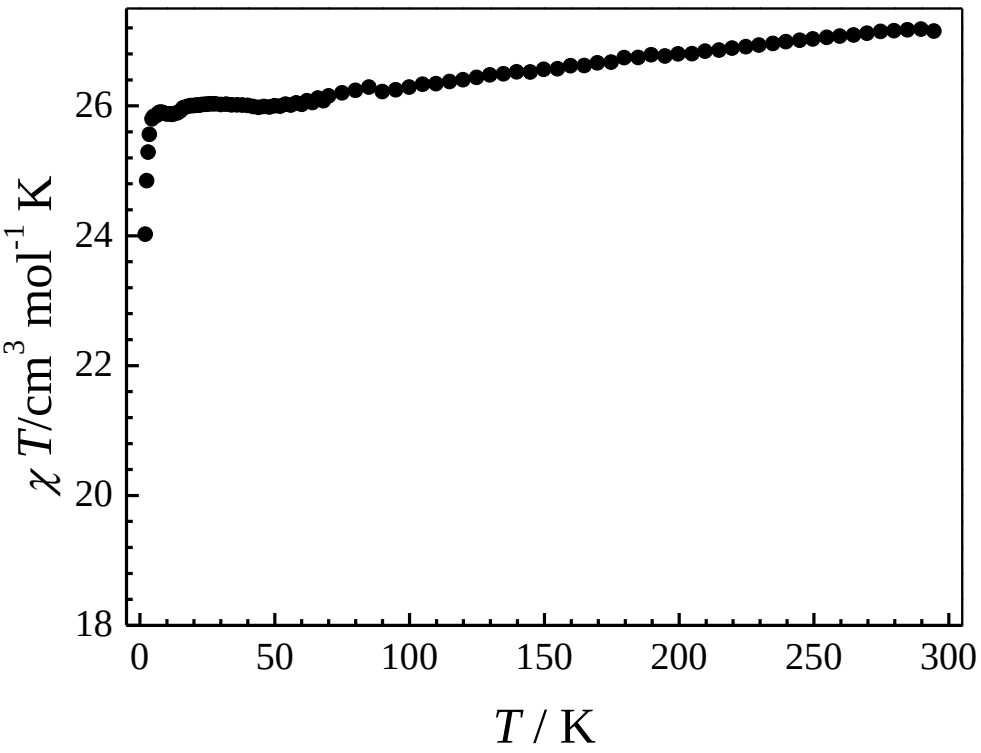

Fig. S6 Temperature dependence of $\chi_M T$ from 300-2K for **2** measured in a field of 2000 Oe.

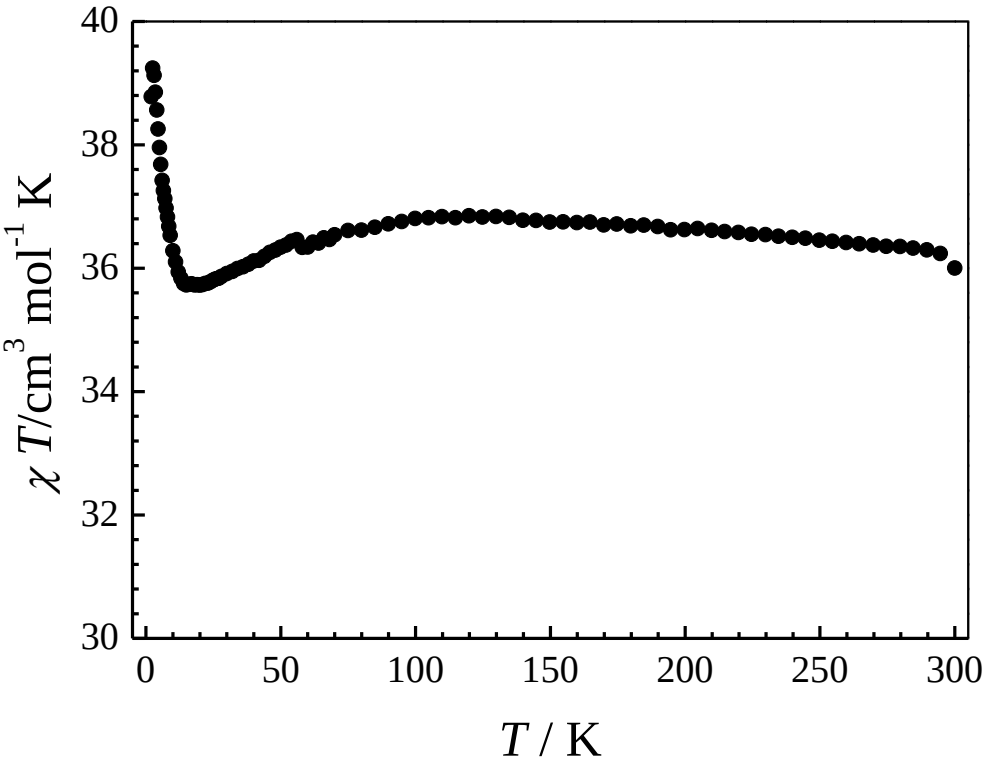

Fig. S7 Temperature dependence of $\chi_M T$ from 300-2K for **3** measured in a field of 2000 Oe.

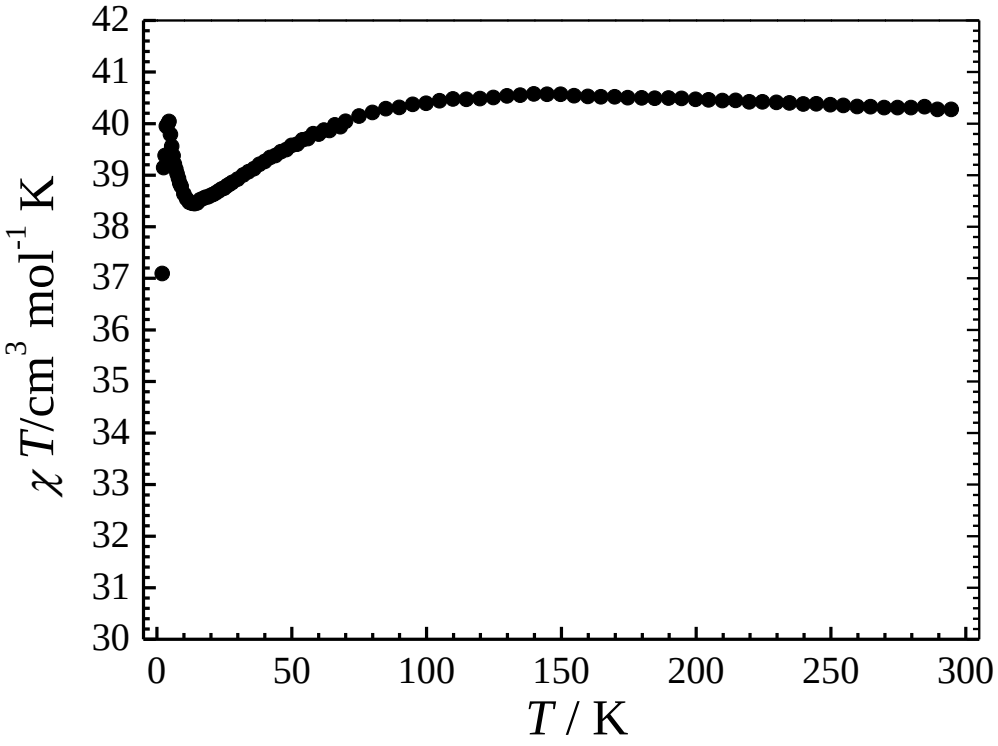

Fig. S8 The $\chi_M T$ versus T plot of **4** under 2000 Oe dc field

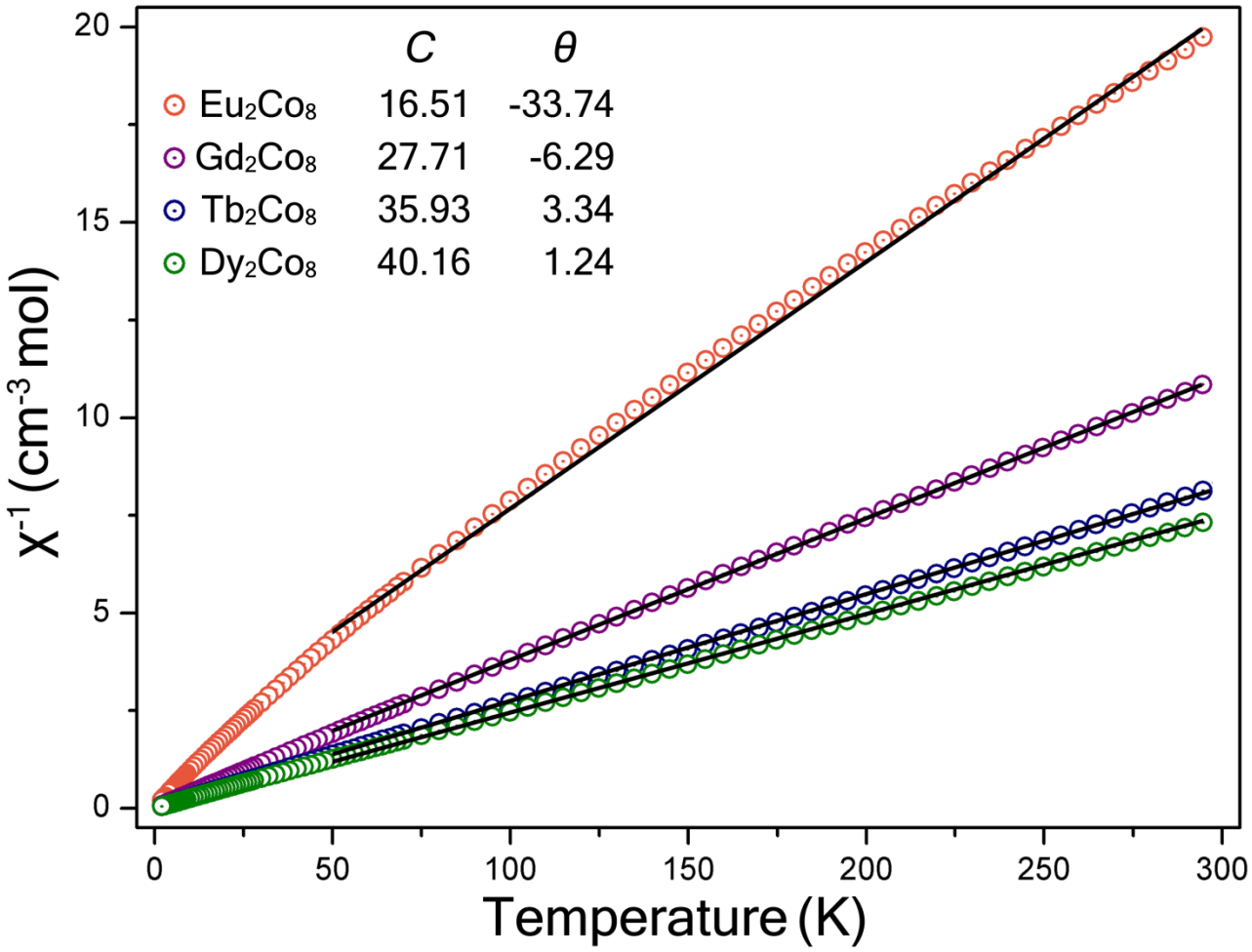

Fig. S9 The χ_m^{-1} versus *T* plots and Curie-Weiss fitting of **1**-**4**.

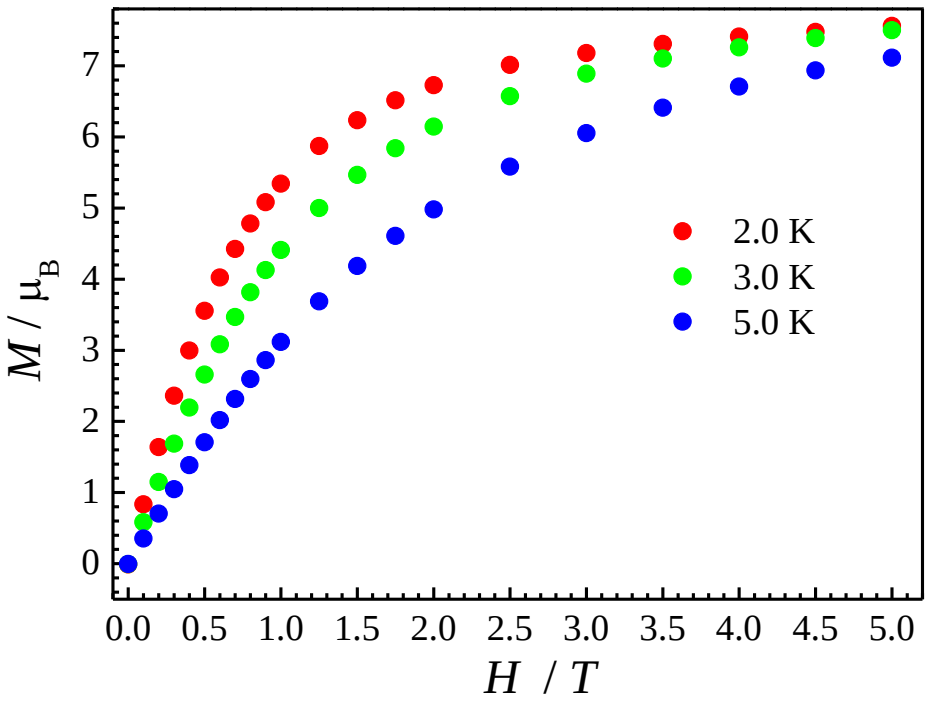

Fig. S10 Isothermal magnetization curves for **1** collected from 2 K to 5 K.

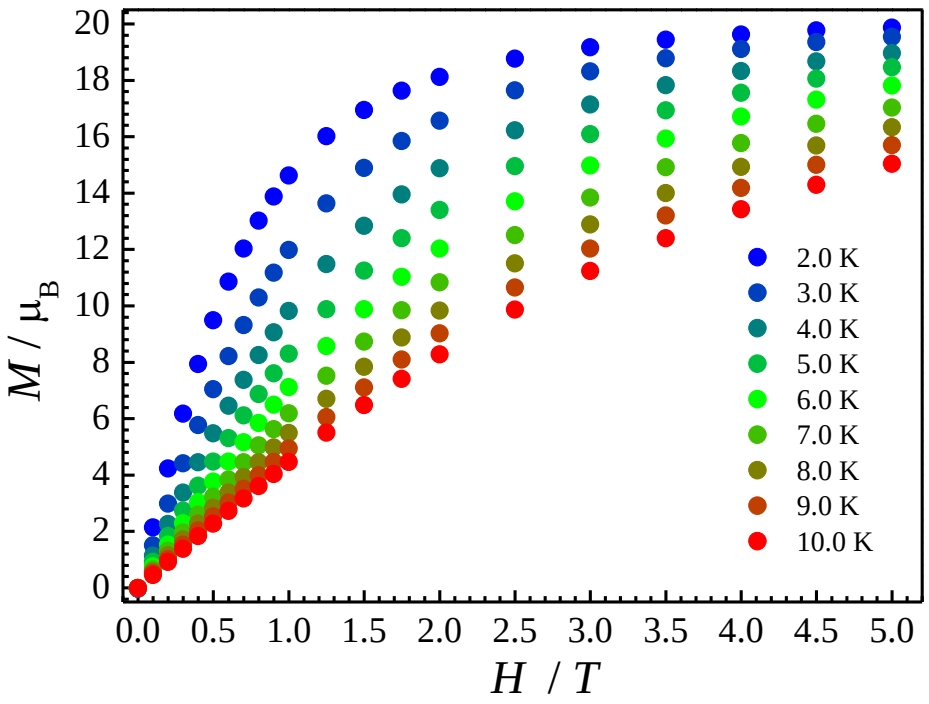

Fig. S11 Isothermal magnetization curves for **2** collected from 2 K to 10 K.

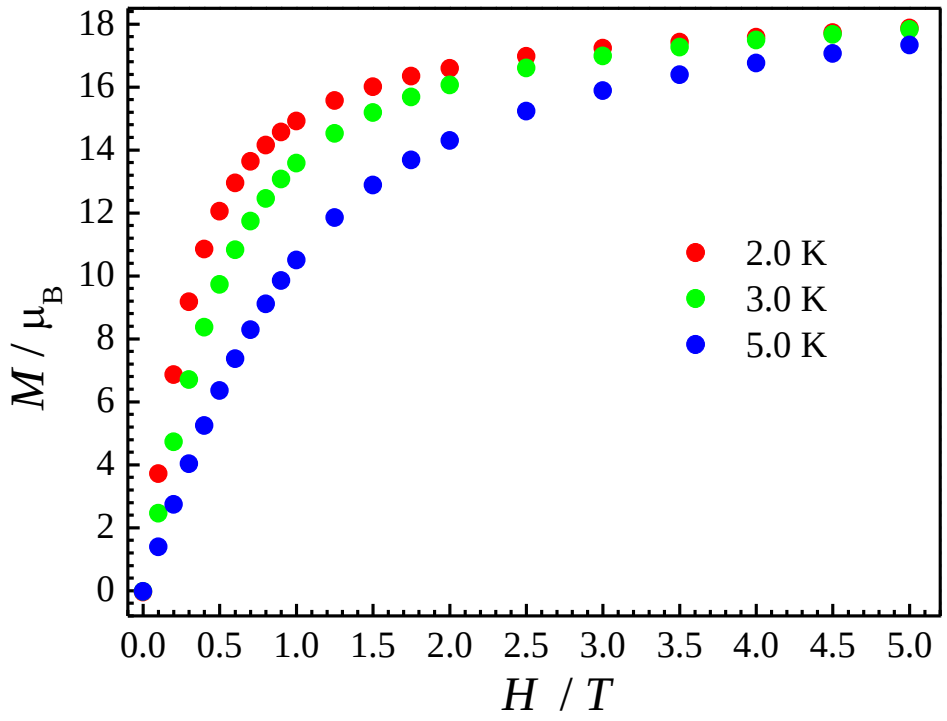

Fig. S12 Isothermal magnetization curves for **3** collected from 2 K to 5 K.

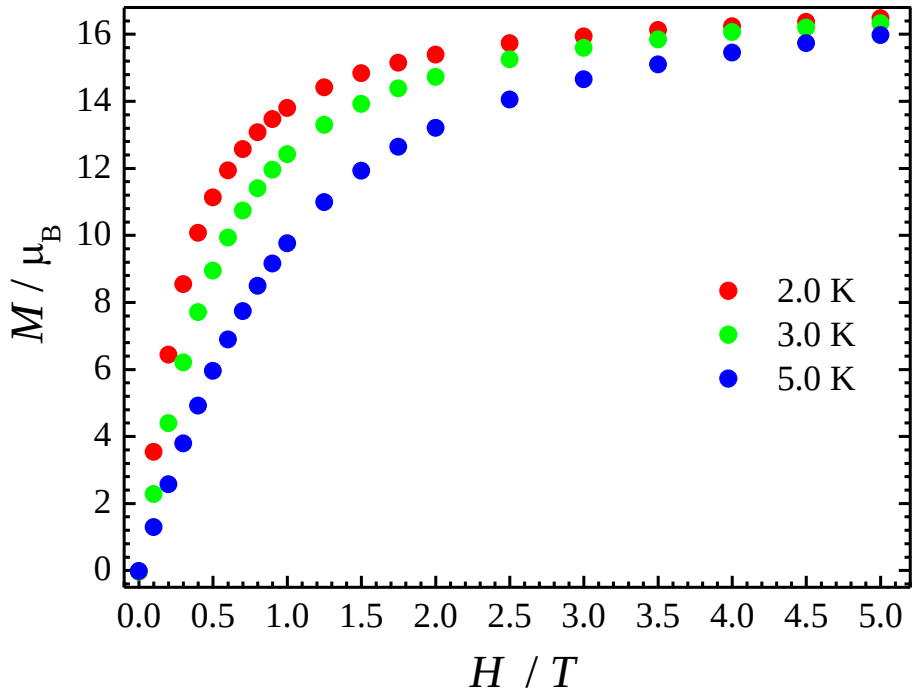

Fig. S13 Isothermal magnetization curves for **4** collected from 2 K to 5 K.

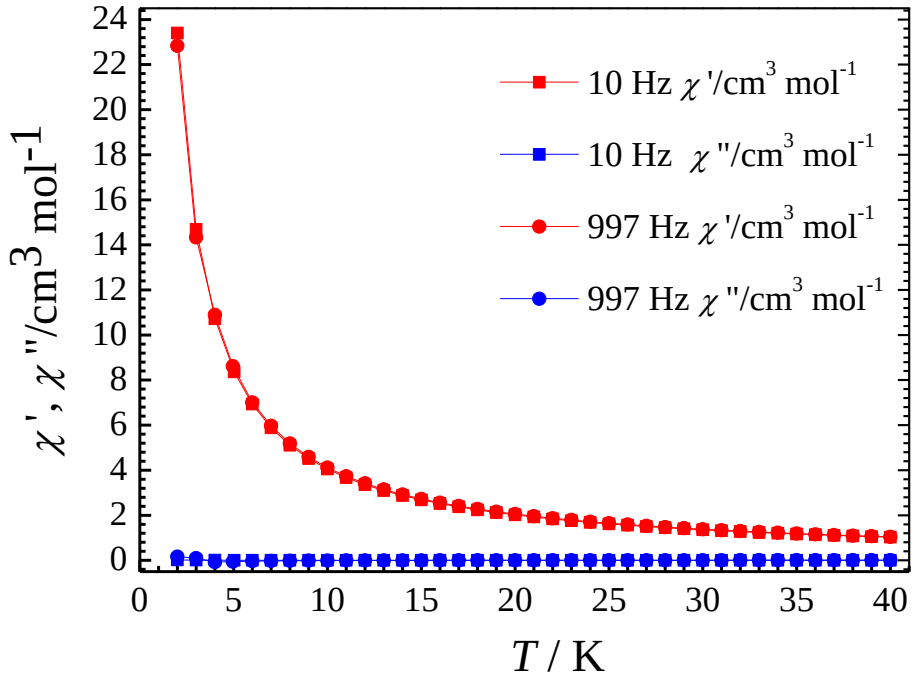

Fig. S14 AC susceptibility measurement for **4**.

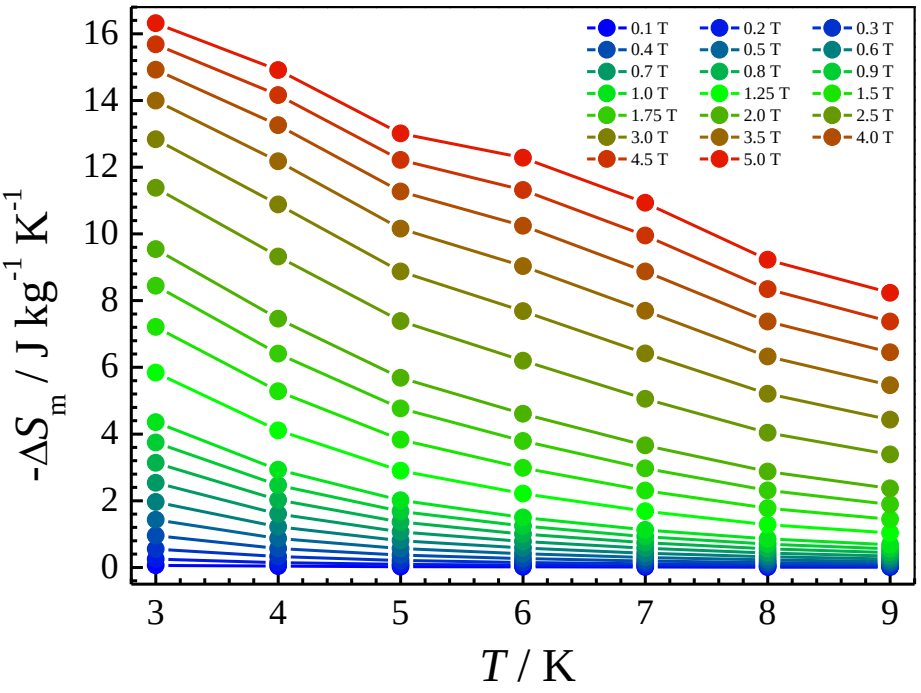

Fig. S15 The plots of $-\Delta S_m$ for **2**.